

Reply to Reviewer 2

We thank the reviewer for reviewing our manuscript and providing comments, questions, food for thoughts, and corrections. We went through all points and provide answers to each of them. Where necessary, we also modified the manuscript. Please see below for the details.

Specific comments:

MIPAS-simulations: To be able to estimate how much the instrumental performance itself contributes to the cloud/aerosol top height estimation, it would be interesting to estimate/discuss the errors introduced by the random and systematic uncertainties of MIPAS, e.g. spectral noise, radiometric accuracy, and others as described by Kleinert et al., 2018.

Indeed, our manuscript did not include a discussion on the impact of the instrument errors on the cloud detection. As we have not presented our considerations in the submitted version, we added a subsection 3.3 and a new Fig. 3 on this topic to Section 3 in the revised manuscript.

“3.3 Error estimation”

“The idealised simulations above do not contain any instrument errors. To assess the potential impact of MIPAS instrument errors on the cloud detection with the ACI, we compared the increase in radiance due to aerosol/clouds with the average noise equivalent spectral radiance (NESR) of $2 \times 10^{-4} \text{ W m}^{-2} \text{ sr}^{-1} \text{ cm}$ for the optimised resolution mode, the total scaling accuracy of 2.4 %, and the total offset accuracy of $9.5 \times 10^{-5} \text{ W m}^{-2} \text{ sr}^{-1} \text{ cm}$ for band A (Kleinert et al., 2018). Although by absolute value the NESR appears to be the largest error it is reduced by \sqrt{n} , because we averaged over $n = 17, 34,$ and 129 spectral points in the three ACI windows respectively. The exemplary selected profiles for the three windows in Fig. 1 show that the increase in radiance at cloud top altitude is well above the NESR and the offset error, while the scaling accuracy results in a very tight envelope around the increase in radiance. From this consideration we deduced that using an ACI value above 7 ensures that no instrument effects are accidentally interpreted as a cloud. Moreover, Fig. 1 shows that the particle size distribution causes a significant spread of the increase in radiance (for ice clouds, sulphate aerosol, and ash with $\beta_e = 1 \times 10^{-3} \text{ km}^{-1}$ the spread at cloud top is $6.9 \times 10^{-3}, 7.5 \times 10^{-4},$ and $1.1 \times 10^{-3} \text{ W m}^{-2} \text{ sr}^{-1} \text{ cm}$, respectively), and hence can be considered an important source of variability.”

Could you discuss whether it would make sense with respect to detection sensitivity, to use the radiances at the maximum of the sulfate peak around 1100 cm⁻¹ instead of those around 800 cm⁻¹ for the aerosol detection since the absorption seems to be an order of magnitude higher?

The main reason for not selecting a window in band AB (1020–1170 cm⁻¹) is that we did not find a useful window there. Comparing the radiance contour plot of a non-cloudy profile for band A (Fig. 2a) with band AB (Fig. 2b), the window regions around 832 cm⁻¹ and 960 cm⁻¹ clearly stand out with low radiances (dark colours) even at

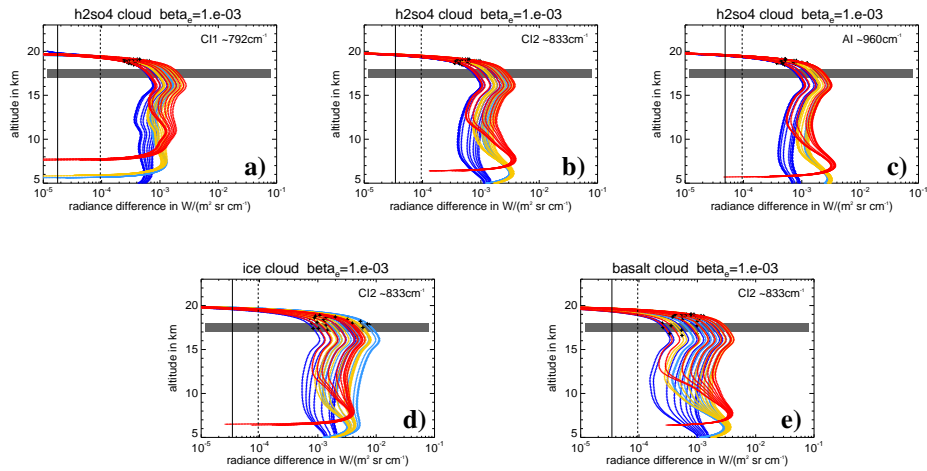


Figure 1: Increase in radiance (cloud – clear air simulation) due to different clouds (solid coloured lines) compared to NESR (black solid line), offset accuracy (black dashed line), and scaling accuracy (dotted coloured lines; very close envelopes around solid coloured lines) for sulphate aerosol in a) the CI window around 792 cm^{-1} (CI1), b) the CI window around 833 cm^{-1} (CI2), c) the AI window around 960 cm^{-1} , and d) for ice, e) and ash. The colours indicate the background atmosphere type: red - tropics, yellow - mid-latitudes, light blue - polar summer, dark blue - polar winter. Each line represents one particle size distribution. The black symbols indicate the detected cloud top altitude using $ACI=7$.

the lowest altitudes. In contrast, in band AB there is no obvious window region. In the entire band AB O_3 has a strong impact, which actually impairs relatively weak aerosol signals at altitudes below the ozone layer. Further, there are contributions by other species, such as CO_2 , CFC-11, CFC-12, HCFC-22, N_2O , that also interfere with UTLS aerosol signals.

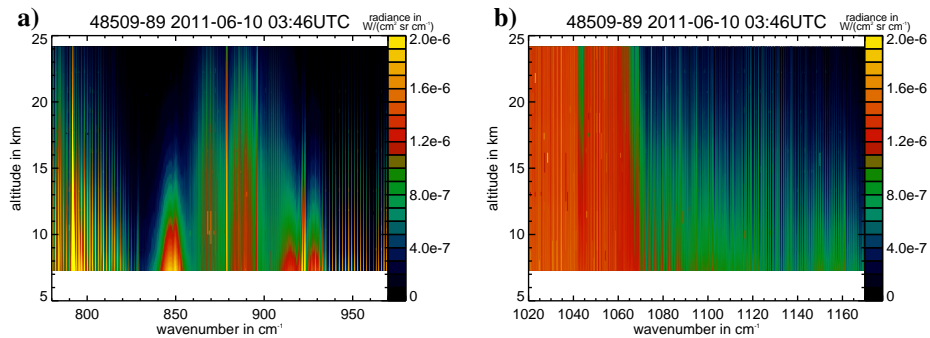


Figure 2: Radiances of a clear air profile in a) band A and b) band B.

Regarding the comparison with CALIOP: could the variability of the CALIOP aerosol top height within the match-criteria be used to estimate the plume's homogeneity at its upper level and be correlated with the MIPAS cloud-top in order to distinguish between cloud-inhomogeneity and optical thickness as the reason for the underestimation by MIPAS?

In our study the CALIOP data are already averaged over 1° , corresponding to 111 km, to achieve a sufficient detection sensitivity for the comparison with MIPAS. Hence, a lot of variability in the CALIOP data is already smoothed out. Fig. 3a shows that the standard deviation decreases over time, which can be expected for an aging aerosol plume. The top altitude difference shows only a slight dependency on the standard deviation of the CALIOP aerosol top height (Fig. 3b) and thus cannot be used to distinguish between cloud-inhomogeneity and optical thickness as the reason for the underestimation by MIPAS.

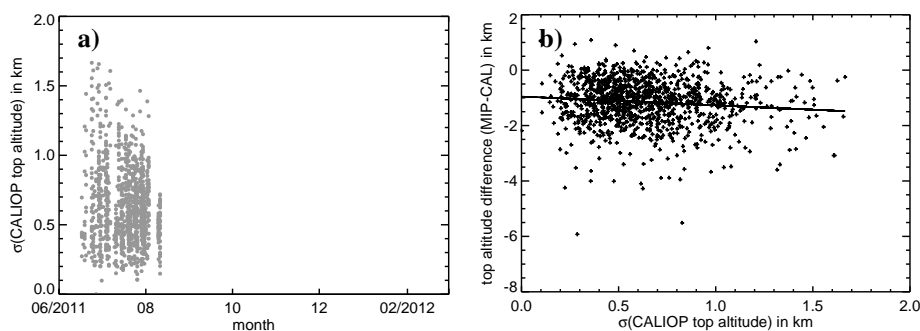


Figure 3: Standard deviation σ of the CALIOP aerosol layer top height within the MIPAS match radius a) Evolution of σ with time b) top altitude difference between MIPAS and CALIOP aerosol detections as a function of σ .

Throughout the paper it is argued with extinction. However, would a quantity like optical depth covered by the field-of-view not be better suited?

Yes, we thought so too and investigated if a 3D equivalent to AOD (path length in cloud \times extinction), the aerosol optical volume ($AOV = \text{integrated FOV along the line of sight in cloud} \times \text{extinction}^3$) would be a better parameter. We started with a 2D setup and integrated the vertically oriented area filled with cloud for each tangent point (Fig 4a). In the following we used only the tangent heights of the detected cloud top heights. To extend the area to a (3D) volume, we assumed the 3D FOV as a rectangular tube and multiplied the area by 30 km. Fig 2a in the revised manuscript and Fig. 4b in the reply show the integrated FOV-volume along the LOS at the detected cloud top as a function of cloud extinction. Analogously to AOD we then calculated the AOV. In contrast to the expectation that the AOV at cloud detection should be around a constant value, the AOV at the detected cloud top shows an exponential dependency on extinction (Fig. 4c). Using AOV instead of extinction in Fig. 4d gives a very similar picture to Fig. 1b in the manuscript. Since the extinction is the dominant factor and allows for a better comparison with the full suite of other instruments, we prefer presenting the results as a function of extinction.

L534-542: It should be made clear that these considerations are valid for the typical size distribution of sulfate aerosols. Could you also consider/discuss cases for other particle sizes (e.g. smaller particles) where scattering in the UV/VIS is decreased but the absorption signal in the mid-IR is not/less affected?

To make it clearer that these considerations are only valid for sulfate aerosol, we added a scaling curve for stratospheric background aerosol at 20 km (Deshler et al., 2003,

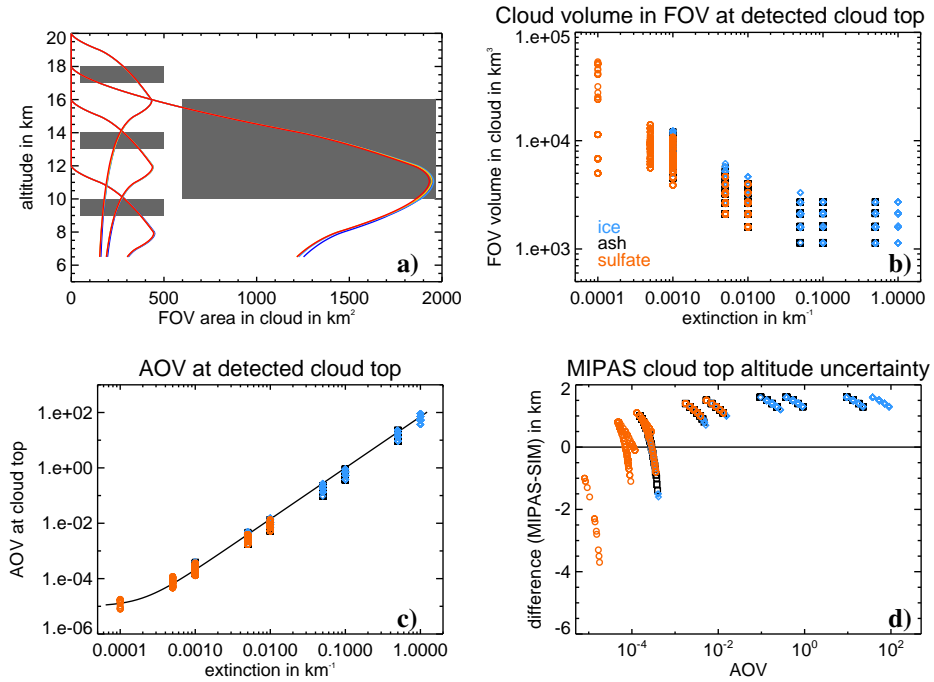


Figure 4: Extinction and field of view diagnostics. a) FOV area filled with cloud as a function of tangent altitude for the simulation scenarios. The grey region indicate the vertical cloud extent. The coloured lines (atmosphere) give the area in cloud for each tangent altitude. b) FOV volume integrated along the line of sight in cloud. Same as Fig. 1a in the manuscript. c) Aerosol optical volume (AOV) at detected cloud top altitude as a function of extinction. d) Cloud top altitude difference as a function of AOV.

($r_{\text{eff}} = 0.13 \mu\text{m}$)), which is very similar to the “Nabro” scaling curve, to Fig. 4 in the revised manuscript and we added to the text:

“... we used the scaling factors for background aerosol and volcanically enhanced sulphate aerosol with particle sizes larger than $0.1 \mu\text{m}$ from Fig. 2 and Table 3 to compare the sensitivity range of MIPAS ...”

and to the figure caption:

“... and background aerosol at 20 km (black solid line Deshler et al., 2003, April 1999).“

For smaller particles the scaling factor from mid-IR to UV/VIS would be lower. However, we did not consider smaller particle sizes than the Deshler measurements indicate for the background state. In Griessbach et al. (2014, Tab. 5) we found that for particle size distributions with effective radii smaller than 100 nm unrealistically high number concentrations are required in order to achieve extinctions that are detectable by MIPAS. Also, for SAGE II Thomason et al. (2008) found a “lack of sensitivity to particles with radii less than 100 nm”. Since the satellite measurements compared here do not have sufficient sensitivity to these smaller particles, which no doubt exist in the UTLS (e.g. Clarke and Kapustin, 2002), we refrained from adding this discussion to the paper.

Table 1: SCIAMACHY and OMPS NPP may be added. The first one since it could be

directly compared to MIPAS in future work and the second to cover the present time and the future.

Thanks for the suggestion. We initially started a more comprehensive Tab. 1 including way more instruments. But as this study is not meant as a satellite aerosol remote sensing review, we decided to include only one representative instrument for each measurement principle. The aerosol measurements of SCIAMACHY and OMPS/LP both rely on the solar scattering technique as OSIRIS, which is still measuring. Studies on OMPS/LP by e.g. Jaross et al. (2014); Flynn et al. (2007) point out the similarities to OSIRIS and SCIAMACHY. Please find below the values we compiled for SCIAMACHY and OMPS/LP. As you will notice, for SCIAMACHY and OMPS/LP we could not find out all values for the parameters we are listing in Tab. 1 in the manuscript. We finally selected OSIRIS, because we could not find conclusive values (on the sensitivity range in particular) for SCIAMACHY and OMPS/LP in literature.

Table 1: Overview of relevant instrument characteristics for global aerosol measurements that also rely on the solar scattering technique as OSIRIS, which we selected as a representative in the manuscript.

instrument	channel	sensitivity range	vertical sampling	coverage	profiles per day	comments & references
OMPS/LP	675 nm ¹	min: max:	1 km ²	82°N–82°S ¹	~ 7000 ²	daytime extinction profiles ¹ Chen et al. (2018); extinction range in figures: $1 \times 10^{-5} - 1 \times 10^{-2} \text{ km}^{-1}$ ² Rault and Loughman (2013)
SCIAMACHY	750 nm ³	min: max:	3.3 km ³	~82°N–82°S ⁴ winter hemisphere ⁵ : 50–60°S; 60–70°N	320– 430 ^{6,7}	daytime extinction profiles ^{3,4,5,6,7} (Rieger et al., 2018; Bovensmann et al., 1999; Weigel et al., 2016; Kaiser et al., 2004; Cardaci, 2010) upper aerosol limits (cloud filtering) extinction range in figures: $1 \times 10^{-5} - 1 \times 10^{-2} \text{ km}^{-1}$ (Taha et al., 2011)

Technical comments:

L50: 'occultation' – > 'occultation' Done.
L69: why is 'However' used here? Removed.
L125: 'color' vs. Figure 1 caption: 'colours', please harmonize Done.
L269: 'maximal' – > 'maximum' Done.
L306: 'compareable' – > 'comparable' Done.
L416: delete ')' Done.
L417: 'analysed' but also 'analyzed' is used Done.
L445: 'dicrepancy' – > 'discrepancy' Done.
L450: 'exinction' – > 'extinction' Done.
L562: 'contradicory' – > 'contradictory' Done.
L659: 'underestimated' – > 'underestimated' Done.
L679: 'soon be available': is the dataset already available?
It is now online (since 6 November 2019).
Table1, last column: ' $1.5 \text{ km}^{-4} \text{ sr}^{-1}$ ' – > ' $1.5^{-4} \text{ km}^{-1} \text{ sr}^{-1}$ ' Fixed.
Fig. 5, caption: 'inidcated' – > 'indicated' Done.

Fig. 9: could you also show a further panel with the absolute plume altitudes to better judge the difference compared to the absolute value. Fig. 9: a legend, e.g. in one of the panels indicating the different instruments would be better than only having the information in the caption.

We added a panel to Fig. 9 (Fig. 11 in the revised manuscript) showing the absolute plume tops measured by MIPAS and the plume altitude (from top to bottom) measured by the lidar and twilight measurements. To this panel we also added the instrument names/ground station names in the corresponding colours. In addition we changed the figure caption to: "Properties of the Nabro sulphate aerosol as a function of time derived from MIPAS (light green), CALIOP (grey), Leipzig lidar (light blue), Jülich lidar (dark blue), Esrange lidar (black), and twilight measurements (dark green). ... a) Nabro aerosol layer height measured by all instruments. For MIPAS only the top height is shown. In case of multiple matches for MIPAS the minimum, maximum, and mean top heights derived are shown. ...", and also refer to the new panel a from the text, where appropriate: "In the comparison of the top heights (Fig. 9a) we see a decrease with time and when moving from low (CALIOP and twilight) to high latitudes (ground based lidars). Compared to the Leipzig lidar measurements ...".

Fig. 13, caption: 'gray' – > 'grey' Done.

References

- Bovensmann, H., Burrows, J. P., Buchwitz, M., Frerick, J., Noël, S., Rozanov, V. V., Chance, K. V., and Goede, A. P. H.: SCIAMACHY: Mission Objectives and Measurement Modes, *J. Atmos. Sci.*, 56, 127–150, [https://doi.org/10.1175/1520-0469\(1999\)056<0127:SMOAMM>2.0.CO;2](https://doi.org/10.1175/1520-0469(1999)056<0127:SMOAMM>2.0.CO;2), URL [https://doi.org/10.1175/1520-0469\(1999\)056<0127:SMOAMM>2.0.CO;2](https://doi.org/10.1175/1520-0469(1999)056<0127:SMOAMM>2.0.CO;2), 1999.
- Cardaci, M.: ENVISAT-1 Products Specifications, Tech. rep., ESA-ESRIN, URL https://earth.esa.int/c/document_library/get_file?folderId=13020&name=DLFE-621.pdf, 2010.

- Chen, Z., Bhartia, P. K., Loughman, R., Colarco, P., and DeLand, M.: Improvement of stratospheric aerosol extinction retrieval from OMPS/LP using a new aerosol model, *Atmos. Meas. Tech.*, 11, 6495–6509, <https://doi.org/10.5194/amt-11-6495-2018>, URL <https://www.atmos-meas-tech.net/11/6495/2018/>, 2018.
- Clarke, A. D. and Kapustin, V. N.: A pacific aerosol survey. Part I: A decade of data on particle production, transport, evolution, and mixing in the troposphere, *J. Atmos. Sci.*, 59, 363–382, 2002.
- Deshler, T., Larsen, N., Weissner, C., Schreiner, J., Mauersberger, K., Cairo, F., Adriani, A., Di Donfrancesco, G., Ovarlez, J., Ovarlez, H., Blum, U., Fricke, K. H., and Dornbrack, A.: Large nitric acid particles at the top of an Arctic stratospheric cloud, *J. Geophys. Res.*, 108, <https://doi.org/10.1029/2003JD003479>, 2003.
- Flynn, L. E., Sefstor, C. J., Larsen, J. C., , and Xu, P.: The Ozone Mapping and Profiler Suite, in: *Earth Science Satellite Remote Sensing*, edited by Qu, J. J., Gao, W., Kafatos, M., Murphy, R. E., and Salomonson, V. V., p. 279–296, Springer, Berlin, URL <https://doi.org/10.1007/978-3-540-37293-6>, 2007.
- Griessbach, S., Hoffmann, L., Spang, R., and Riese, M.: Volcanic ash detection with infrared limb sounding: MIPAS observations and radiative transfer simulations, *Atmos. Meas. Tech.*, 7, 1487–1507, <https://doi.org/10.5194/amt-7-1487-214>, 2014.
- Jaross, G., Bhartia, P. K., Chen, G., Kowitt, M., Haken, M., Chen, Z., Xu, P., Warner, J., and Kelly, T.: OMPS Limb Profiler instrument performance assessment, *J. Geophys. Res.*, 119, 4399–4412, <https://doi.org/10.1002/2013JD020482>, URL <https://agupubs.onlinelibrary.wiley.com/doi/abs/10.1002/2013JD020482>, 2014.
- Kaiser, J., Eichmann, K.-U., Noel, S., Bovensmann, H., Burrows, J., and Frerick, J.: Satellite-pointing retrieval from atmospheric limb-scattering of solar UV-B radiation, *Can. J. Phys.*, 82, 1041–1052, <https://doi.org/10.1139/p04-071>, 2004.
- Kleinert, A., Birk, M., Perron, G., and Wagner, G.: Level 1b error budget for MIPAS on ENVISAT, *Atmos. Meas. Tech.*, 11, 5657–5672, <https://doi.org/10.5194/amt-11-5657-2018>, URL <https://www.atmos-meas-tech.net/11/5657/2018/>, 2018.
- Rault, D. F. and Loughman, R. P.: The OMPS Limb Profiler Environmental Data Record Algorithm Theoretical Basis Document and Expected Performance, *IEEE Trans. Geosci. Remote Sens.*, 51, 2505–2527, <https://doi.org/10.1109/TGRS.2012.2213093>, 2013.
- Rieger, L. A., Malinina, E. P., Rozanov, A. V., Burrows, J. P., Bourassa, A. E., and Degenstein, D. A.: A study of the approaches used to retrieve aerosol extinction, as applied to limb observations made by OSIRIS and SCIAMACHY, *Atmos. Meas. Tech.*, 11, 3433–3445, <https://doi.org/10.5194/amt-11-3433-2018>, URL <https://www.atmos-meas-tech.net/11/3433/2018/>, 2018.
- Taha, G., Rault, D. F., Loughman, R. P., Bourassa, A. E., and von Savigny, C.: SCIAMACHY stratospheric aerosol extinction profile retrieval using the OMPS/LP algorithm, *Atmos. Meas. Tech.*, 4, 547–556, <https://doi.org/10.5194/amt-4-547-2011>, URL <https://www.atmos-meas-tech.net/4/547/2011/>, 2011.

Thomason, L. W., Burton, S. P., Luo, B.-P., and Peter, T.: SAGE II measurements of stratospheric aerosol properties at non-volcanic levels, *Atmos. Chem. Phys.*, 8, 983–995, <https://doi.org/10.5194/acp-8-983-2008>, URL <https://www.atmos-chem-phys.net/8/983/2008/>, 2008.

Weigel, K., Rozanov, A., Azam, F., Bramstedt, K., Damadeo, R., Eichmann, K.-U., Gebhardt, C., Hurst, D., Kraemer, M., Lossow, S., Read, W., Spelten, N., Stiller, G. P., Walker, K. A., Weber, M., Bovensmann, H., and Burrows, J. P.: UTLS water vapour from SCIAMACHY limb measurements V3.01 (2002–2012), *Atmos. Meas. Tech.*, 9, 133–158, <https://doi.org/10.5194/amt-9-133-2016>, URL <https://www.atmos-meas-tech.net/9/133/2016/>, 2016.